Biosynthesis of Bimetallic Ag-Au (core-shell) Nanoparticles Using Aqueous Extract of Bay Leaves (*Laurus nobilis L.*)

Numan Hoda[1]* ✉ iD **, Leyla Budama Akpolat[2]** iD **, Firdevs Mert Sivri[3]** iD **,
and Duygu Kurtuluş[4]** iD

[1.] *Akdeniz University, Department of Material Science and Engineering 07058 Antalya, Turkey*
[2.] *Akdeniz University, Department of Chemistry 07058 Antalya, Turkey*
[3.] *Suleyman Demirel University, Department of Basic Pharmaceutical Sciences, 32200 Isparta, Turkey*
[4.] *Gebze Technical University, Department of Nanoscience and Nanoengineering 41400 Kocaeli, Turkey*

Abstract: The green synthesis of bimetallic nanoparticles using plant extracts is attracting an increasing attention in the nanoparticle production field since, besides being available for the production of bimetallic nanoparticles, it is cost-effective, eco-friendly, and it is available for large scale production. The required agents to reduce and stabilize metal nanoparticles during synthesis already exist in plant extracts as phytochemicals. The study highlights the synthesis of gold, silver, and silver-gold (bimetallic) nanoparticles at room temperature using an aqueous extract of dried bay leaves and their physical and chemical characterizations for their potential applications. We have synthesized Ag, Au, and Ag-Au nanoparticles using the aqueous bay leaves extract. The nanoparticles were characterized by UV-Vis spectroscopy, X-ray diffraction (XRD), transmission electron microscopy (TEM), and Fourier transform infrared spectroscopy (FT-IR). According to UV-Vis spectroscopic results, it is concluded that Ag-Au bimetallic nanoparticles synthesized in the extract have a core-shell arrangement. XRD measurements revealed that all nanoparticles (Ag, Au, and Ag-Au) are in fcc structure. The nanoparticles' average sizes were measured as 10±7, 23±4, and 8±3 nm for Ag, Au, and Ag-Au nanoparticles, respectively, as determined from the TEM images. The results offer that besides Ag and Au nanoparticles, bimetallic Ag-Au nanoparticles synthesized in an aqueous extract of dried bay leaves may play a prominent role in the field of nanotechnology, especially in nanomedicine.

*Corresponding author. E-mail: nhoda@akdeniz.edu.tr.

INTRODUCTION

Bimetallic nanoparticles often display different or better catalytic, optical and magnetic properties and surface energy than their monometallic counterparts due to the synergism between two metallic nanoparticles (1–4). These nanoparticles' structures can be divided into alloys and core-shell structures (5). Alloy structure may be defined as merely a "mixture of at least two different metal atoms in one nanoparticle," and core-shell structure consists of nanoparticles having a monometallic core surrounded by another metallic layer (shell) (Figure 1). Among core-shell nanoparticles, the Au-Ag combination is one of the most studied bimetallic nanostructures due to their surface plasmon resonance (SPR) tunability features for applications such as sensing, imaging, and nanophotonics (5–8). Ag–Au core-shell nanoparticles can be prepared by a number of

methods such as seed-growth (9,10), pulsed laser ablation (11), green approach (12,13), etc. Among them, green approach is one of the emerging fields in nanoscience and nanotechnology, because of being eco-friendly, biocompatible, low-cost, and energy-efficiency (13–16). There are many publications on the synthesis of bimetallic nanoparticles of Au-Ag using plant extracts such as Neem (*Azadirachta indica*) leaf broth (14), Persimmon (*Diospyros kaki*) leaf (17), *Anacardium occidentale* (18), mushroom (13), mahogany (Swietenia mahogani JACQ.) leaf (19), *Cacumen platycladi* leaf (20), cruciferous vegetable (21), *piper pedicellatum* (22), and sago pondweed (*Potamogeton pectinatus* L.) (23). The synthesis of nanoparticles in plant extracts is a bottom-up approach in which metal salts are used as precursors. Biomolecules present (carbohydrates, proteins, sugars, etc.) can be responsible for reducing metal ions into metal nanoparticles. For example, Mondal et al. (19) reported that bimetallic Au-Ag nanoparticles were produced using mahogany leaf extract. Also, they claimed that limonoids, one group of the phytochemical constituents of the mahogany leaf, were reducing and stabilizing agents for the formation of stable nanoparticles. Bimetallic nanoparticles are synthesized by simultaneous or sequential reduction in plant extracts. In simultaneous reduction, two metal ions are added into plant extract together (co-reduction), leading to the formation of alloy or core-shell structure (14,19). Sequential reduction involves the addition of two metal ions into plant extracts successively, and it is the most promising method to synthesize core-shell bimetallic nanoparticles. In this method, one of the two metal ions is added first and reduced to form nanoparticle as core and second metal ions are deposited by reduction onto preformed nanoparticle (core) to form shell. While there are limited publications concerning synthesis of Ag-Au (core-shell) structured bimetallic nanoparticles using plant extracts in literature (24), there are many researches on the synthesis of Au-Ag (core-shell) or alloy structured bimetallic nanoparticles using plant extracts (14,17,18). Ag-Au (core-shell) bimetallic nanoparticles are used in many applications such as a sensing and medical imaging etc. (25,26). Therefore, it is worth studying the synthesis of Ag-Au (core-shell) bimetallic nanoparticles that are biocompatible, in green and eco-friendly way.
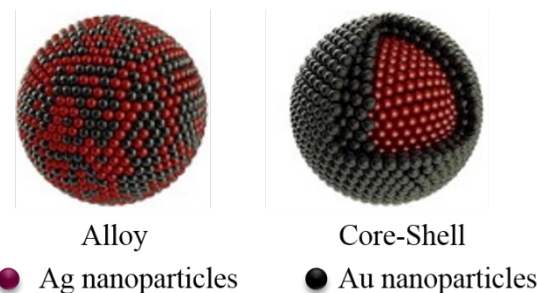
Figure 1: A schematic representation of alloy and core-shell structure of bimetallic nanoparticles.

Laurus nobilis L., commonly known as bay leaves, is a Laureacea family member, being one of the native species to the Mediterranean region (27). It is an evergreen tree cultivated in many countries with the moderate and subtropical climax, such as Italy, Turkey, Mexico, Spain, and the USA (28). It can also be used as a spicy fragrance and flavor in traditional dishes (29); it is also used to treat the symptoms of gastric secretion, flatulence, and rheumatic complaints (30). Aqueous extract of bay leaves contains constituents such as sugars, organic acids, acylated kaempferol glycosides, sesquiterpene lactones, megastigme glycosides, (+)-catechin, (-)-epicatechin, (+)-gallocatechin, (+)-epigallocatechin, and procyanidins (B2, B4, B5 and B7, etc.), which can reduce metallic ions to form nanoparticles and stabilize them (31–36). A few researches on the synthesis of nanoparticles using bay leaves extract are seen in literature in the last few years (37–39). For example, Vijakumar et al. (2016) synthesized ZnO nanoparticles using aqueous bay leaves extract and characterized them by UV–Vis spectroscopy, FTIR, XRD, TEM, SEM, and EDX. After characterization, they further investigated ZnO nanoparticles synthesized for their antibacterial activity, cytotoxicity, and anticancer activity. They found that ZnO nanoparticles synthesized effectively inhibited the biofilm growth of *S. aureus* and *P. aeruginosa* at 75 mg.mL^{-1}, showed no cytotoxic effect on normal murine RAW264.7 macrophage cells, and were influential in inhibiting the viability of human A549 pulmonary cancer cells at higher concentrations of 80 mg.mL^{-1}. The present work's primary purpose is to synthesize Ag, Au, and bimetallic Ag-Au nanoparticles using aqueous bay leaves extract and characterize them for their further applications. There is no publication on the synthesis of Ag-Au bimetallic nanoparticles using bay leaves extract to the best of our knowledge.

EXPERIMENTAL

Material and Method
Silver nitrate, AgNO$_3$ (Aldrich), and sodium tetrachloroaurate(III) (NaAuCl$_4$.2H$_2$O) were used as purchased. In the extraction processes,

Hoda N et al. JOTCSA. 2021; 8(4): 1035-1044.

RESEARCH ARTICLE

deionized water was used. All other reagents were purchased from commercial sources and were used after the usual drying and/or distillation without further purification. Bay leaves were purchased from the local market and confirmed that they are gathered in the Mediterranean coast of Antalya, Turkey, and dried in shadow.

Preparation of aqueous leaves extract

After washing with tap water, the leaves were washed twice with deionized water and spread to dry for three days at room temperature and ground. The ground leaves were sieved, and the fraction of 0.650-1.00 mm was used for extraction. 2.5 gram of leaves powder was taken into an Erlenmeyer flask, and 100 mL of deionized water was added and then refluxed for 5 min. After cooling to room temperature, the mixture was sieved with 0.350 mm mesh to remove large

particles, and then it was centrifuged with 4500 rpm for 15 min. The supernatant was collected and stored at 4 ºC for further studies.

Synthesis of nanoparticles

0.01 M, 1 mL of $AgNO_3$, and $HAuCl_4$ were added to 10 mL of extracts to synthesize Ag and Au nanoparticles separately, and the mixtures were stirred for 24 h in a dark condition at room temperature. For the synthesis of Ag-Au core-shell nanoparticles, 0.01 M, 1 mL of $AgNO_3$ has initially been added to 10 mL of extract and was allowed to be reduced and stabilized by phytochemicals present in the extract. Then, the corresponding portion of $HAuCl_4$ was added and allowed to complete the reaction. The green synthetic steps of the Au-Ag bimetallic nanoparticles are shown in Figure 2.
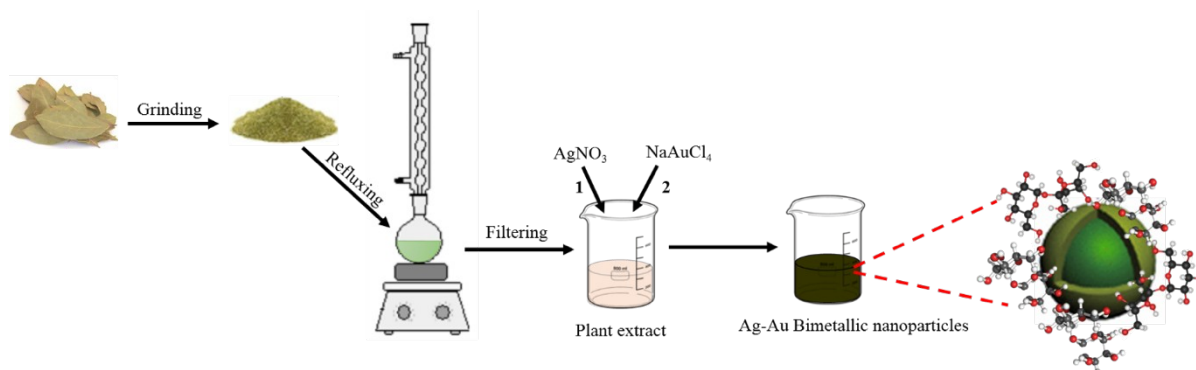
Figure 2: Schematic diagram of green synthesis of Ag-Au bimetallic nanoparticles using aqueous extract of bay leaves (*Laurus nobilis L.*).

Characterization of synthesized nanoparticles

UV-visible spectra of extracts containing Ag, Au, and Ag-Au nanoparticles were recorded with the wavelength range from 200 to 800 nm using a Perkin Elmer Lambda 35 UV/Vis spectrometer operating at a resolution of 1 nm. X-ray (XRD) patterns of synthesized nanoparticles were obtained using Rigaku MiniFlex X-ray diffractometer with monochromatic Cu-Kα incident beam (λ=0.154056 nm) with nickel monochromator the range between 10° and 90° at 2θ angle. The morphologies and the synthesized nanoparticles' sizes were examined through Transmission Electron Microscopy (TEM) Zeiss Leo 906E TEM instrument by evaluating TEM images with Adobe Photoshop 7. A total of 200 particles were counted and averaged for corresponding particle sizes. Fourier transforms infrared (FT-IR) spectra were recorded with ATR-FTIR using Perkin Elmer Two spectrometer at room temperature at 4 cm^{-1} resolution.

RESULTS AND DISCUSSION

The synthesis of Ag, Au, and Ag-Au (core-shell) nanoparticles was performed in an aqueous bay leaf extract. After adding any precursor into an extract and stirring, an immediate change in color of solutions was observed, confirming nanoparticles' formation by reduction reactions. As indicated in the inset of Figure 3. the color of extracts turned into dark-yellow, purple, and grayish-black for Ag, Au, and Ag-Au nanoparticles, respectively. Also, Figure 3 shows the UV-Vis spectra of synthesized nanoparticles. The absorption peaks at 425 nm (Figure 3b) and 542 nm (Figure 3c) belong to the SPR absorption of Ag and Au nanoparticles. SPR bands are highly dependent on the shape and size of the nanoparticles (40). The absorption peak observed at 542 nm is the characteristic peak for spherical gold nanoparticles (12).
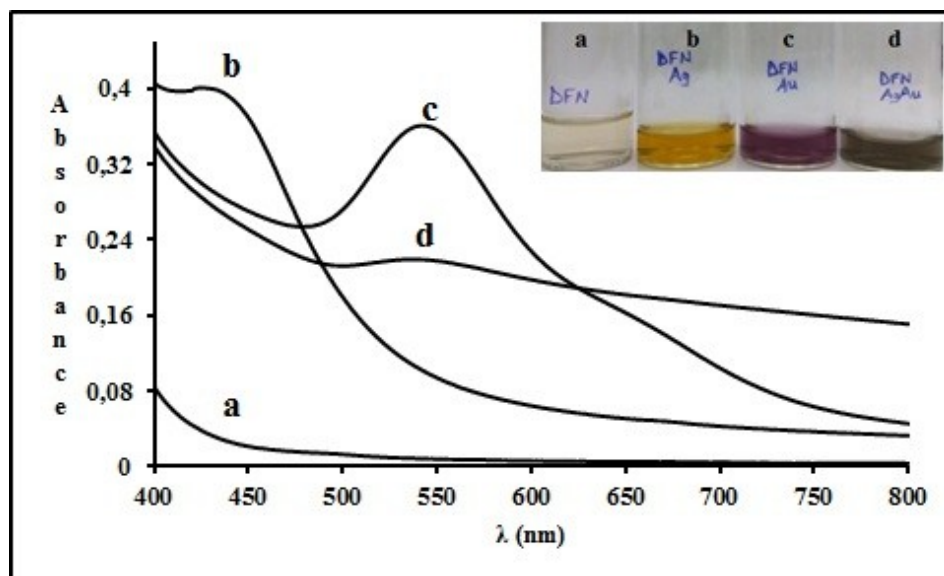
Figure 3: UV spectra of extract and nanoparticle solutions (a, b, c, and d represent bay leaf extract, Ag, Au, and Ag-Au nanoparticles in extract, respectively).

Experimental absorption spectra and calculated spectra for the Au-coated Ag nanoparticles (using full Mie equations and the dielectric data for the alloys) were compared by Mulvaney (41) to investigate whether the optical spectra alone can reveal whether alloying has taken place during deposition of a second metal onto a seed metal particle. According to Mulvaney's work (1996), Ag-Au bimetallic nanoparticles' alloyed structure has a single plasmon band between the corresponding bands of monometallic Ag and Au nanoparticles regarding content ratios of corresponding metals. As Au content increases in the bimetallic nanoparticle, a continuous red-shift in the band position is observed. In the case of core-shell structures (Ag-core, Au-shell) Ag (core) plasmon band is strongly damped but does not shift, and Au's thick coating on the Ag core shows a plasmon band close to the band of monometallic Au nanoparticle. As Au content (correspondingly thickness of the shell) increases, damping in the Ag (core) band increases. In our case for Ag-Au synthesized nanoparticles, the SPR absorption observed at 538 nm (Figure 3d) confirming the Ag-Au bimetallic nanoparticles are in core-shell arrangement. Because, in the UV-Vis spectrum of Ag-Au bimetallic nanoparticles, the disappearance of absorption peak for Ag nanoparticles and still observing absorption peak at almost the same position as in monometallic Au nanoparticles strongly suggest that Ag nanoparticles formed core and Au formed the shell. Also, the complete disappearance of absorption peak for Ag nanoparticles depends on the thickness of the shell since, when the shell is sufficiently thick, only absorption corresponding to shell could be observed, but when the thickness of the shell is not enough to shield UV-Vis waves, any absorption

from the core could occur (41). The results are in good agreement with the works on Ag-Au core-shell bimetallic nanoparticles (12–16,24,27–30,35–38,42). In general, during synthesizing bimetallic nanoparticles of Ag and Au by co-reduction, if monometallic nanoparticles of Au and Ag form separately, the solution will be just a physical mixture of the corresponding nanoparticles; just two absorption bands will be observed at the same position and intensity with the monometallic counterparts. Nevertheless, when any intensity change is observed at the absorption maxima, it can result from the formation of core-shell arrangement. In alloy arrangement for bimetallic nanoparticles, only one absorption peak is observed between two maxima of the corresponding monometallic nanoparticles, and the peak of maximum observed depends on the concentration of the precursors (41,42).

The crystalline natures of the synthesized nanoparticles were confirmed by X-ray diffraction (XRD) analysis. Powders of nanoparticles were obtained by vacuum drying of extracts containing nanoparticles using a rotary evaporator. The XRD patterns of powders are given in Figure 4. As illustrated in Figure 4a, the XRD pattern of Ag nanoparticles shows four distinct diffraction peaks at 38.1°, 43.9°, 64.5° and 77.1° representing (1 1 1), (2 0 0), (2 2 0), and (3 1 1) crystal planes of a faced center cubic (fcc) lattice of silver consistent with the JCPDS data [No. 04-0783]. In Au nanoparticle diffraction pattern (Figure 4b), the peaks at 38.1°, 44.2°, 64.4° and 77.4°correspond to the (1 1 1), (2 0 0), (2 2 0) and (3 1 1) facets (1,28,30,36) of the face-centered cubic crystal structure, respectively. The ratio between peak intensities gives the predominant orientation, and

in the Au nanoparticle diffraction pattern, the ratio of intensities of (2 0 0) and (1 1 1) peaks is much lower than the usual value (0.52), suggesting that the (1 1 1) plane is the predominant orientation (27). In the case of Ag-Au bimetallic nanoparticles (Figure 4c), diffraction peaks appeared at 38.1º (111), 44.1º (200), 64.4º (220), and 77.1º (311),

confirming that Ag-Au bimetallic nanoparticles are in fcc structure. Unassigned peaks in all the XRD patterns can be attributed to the crystallization of the bioorganic phase on nanoparticles' surface. Similar results were reported in some works in the literature, too (12,13,21).
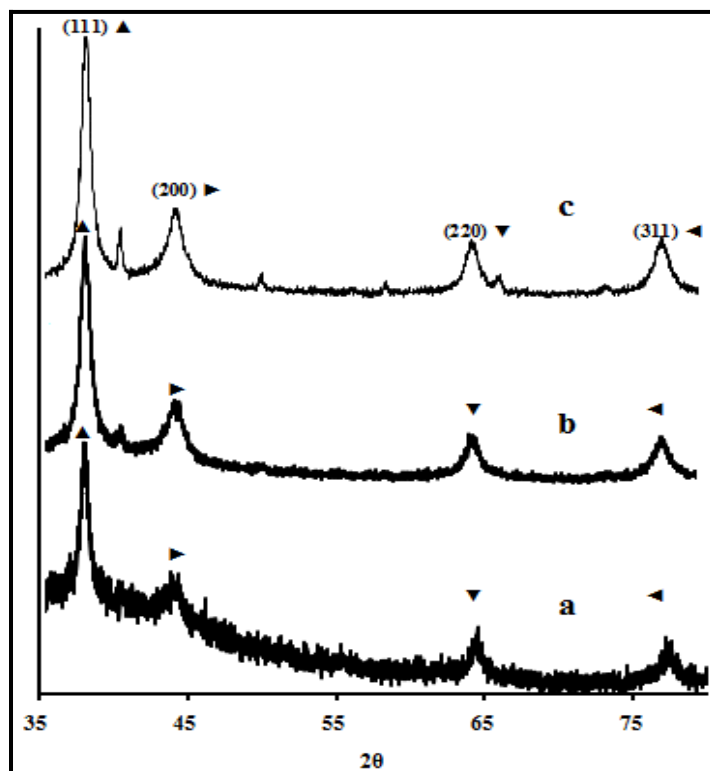
Figure 4: XRD patterns of nanoparticles synthesized (a, b and c represent Ag, Au and Ag-Au nanoparticles, respectively).

The TEM images of nanoparticles synthesized in bay laurel leaves extract are given in Figure 5, and these images can help us analyze the size and shape of the nanoparticles. Figure 5(a), 5(b), and 5(c) are the images of nanoparticles of Ag, Au, and Ag-Au (core-shell), respectively. The shape of the nanoparticles is spherical primarily, but for Au nanoparticles, a few hexagonal and triangular shapes were observed in TEM images not given here. While Ag-Au nanoparticles' size ranges between 1 nm and 17 nm with a mean diameter of 8±3 nm, Au nanoparticles' size ranges between 12 and 33 nm with a mean diameter of 23±4 nm and Ag nanoparticles' size ranges between 1 nm and 31 nm with a mean diameter of 10±7 nm. The size

of core-shell Ag-Au nanoparticles is smaller than that of Au and Ag nanoparticles synthesized. Gopinath et al. synthesized Ag, Au and Ag-Au bimetallic nanoparticles by using the *Gloriosa superba* leaf extract and they reported that mean size of Ag-Au bimetallic nanoparticles as 10 nm (43) which is close to our findings. In another study, Chavez and Rosas synthesized Ag-Au Core-shell bimetallic nanoparticles using the extract of *Hamelia patens* plant and they found that the particle size distribution ranging from 10 to 50 nm being the average particle size was 32 nm (44) which is four folded of our findings. The size of nanoparticles synthesized using plant extracts may depend on plant types.
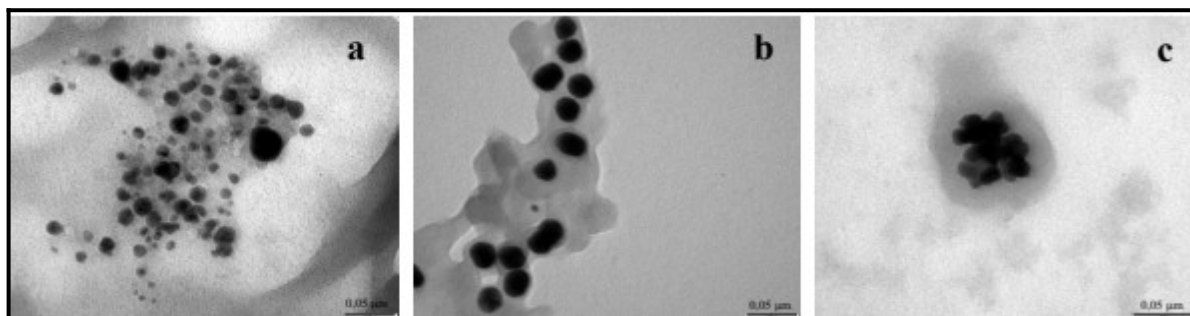
Figure 5: TEM images of the **a)** Ag, **b)** Au, and **c)** Ag-Au nanoparticles in bay leaf extract.

Fourier Transform Infrared Spectroscopy (FT-IR) measurements of pure and nanoparticle-containing powdered samples of bay leaf extract were carried out to identify the possible interactions between the nanoparticles (Ag, Au, and Ag-Au) and bioactive molecules, which might be effective in the synthesis and stabilization of the nanoparticles in the extracts. The FT-IR spectra obtained from the pure extract powders display absorption peaks at different positions for various functional groups at 3342, 2921, 2856, 1711, 1606, 1438, 1373, 1206, 1040, and 775 cm^{-1} as seen Figure 6. The bands at 3342 cm^{-1} and 1040 cm^{-1} can be attributable to O-H stretching vibrations indicating hydroxyl groups' presence in the structure of biomolecules present in the powder of extract (45). The bands observed at around 2921 cm^{-1} and 2850 cm^{-1} are from stretching vibration of C-H (46). The stretching vibrations of the C=O group from ketones are observed at 1722 cm^{-1}. While the

band observed at 1616 cm^{-1} corresponds to stretching of C-O bond of amide-I, the weak band at 1440 cm^{-1} corresponds to –C=C- vibrations from aromatic skeletal compounds (47). The bands at 1373 and 775 cm^{-1} are assigned to C-H bending vibration for –CH_3 symmetrical deformation and N-H's bending vibration, respectively. The band at 1206 cm^{-1} can be attributed to in-plane bending vibration of the –OH group of phenols (48). While the characteristic IR band of amine and amino-methyl stretching groups appeared at 1438 cm^{-1}, -C-N vibrations appeared at 1373 cm^{-1} (49). When the spectrum of pure extract and spectra of nanoparticle-containing powdered extract samples are compared, there are only minor shifts of about ±1-5 cm^{-1} except for the band at 1040 cm^{-1} which shifted to 1032 cm^{-1} for Au and Ag-Au containing samples. As explained above, many functional groups are responsible for reducing or stabilizing the nanoparticles in the extract.
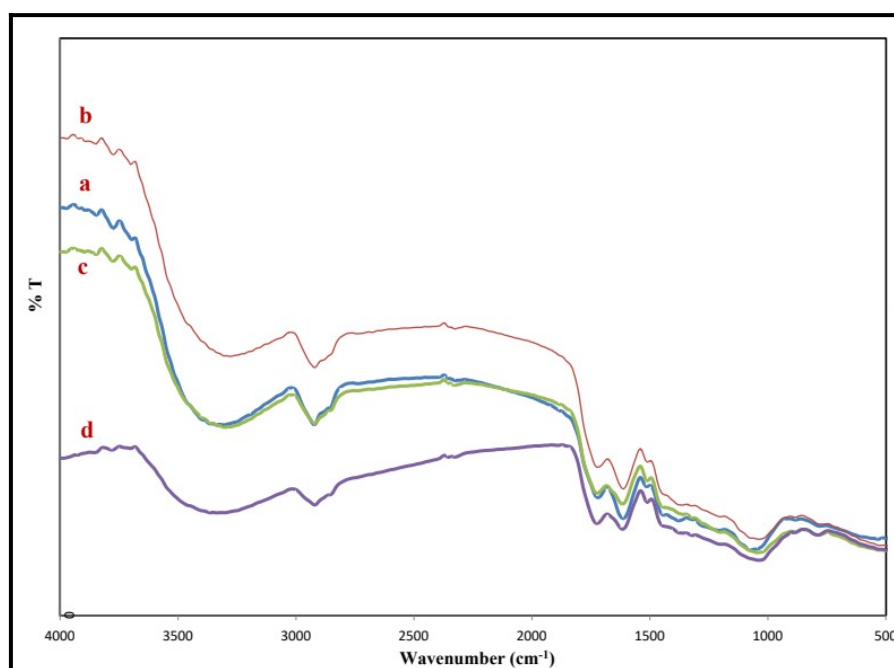
Figure 6: FTIR Spectra of a: bay leaf extract, b: Ag nanoparticles, c: Au nanoparticles, d: Ag-Au bimetallic nanoparticles in the bay leaf extract.

Hoda N et al. JOTCSA. 2021; 8(4): 1035-1044.

RESEARCH ARTICLE

CONCLUSION

This study focused on producing nanoparticles of Ag, Au, and Ag-Au (bimetallic) in the aqueous bay leaf extract. The nanoparticles were prepared by a green, eco-friendly, fast, low cost, and large-scale applicable method. The synthesized nanoparticles were characterized by TEM, UV, XRD, and FT-IR. It was observed that Ag-Au bimetallic nanoparticles synthesized in the extract are in the core-shell structure according to UV spectral results. XRD characterization of nanoparticles showed that all nanoparticles synthesized are in FCC structure. TEM technique was used to identify the size and shape of the nanoparticles. TEM measurements indicated that the nanoparticles' shape is primarily spherical, but a few hexagonal and triangular shapes were observed for Au nanoparticles. The nanoparticles' average sizes were measured as 10±7, 23±4, and 8±3 nm for Ag, Au, and Ag-Au nanoparticles, respectively. FT-IR measurements showed that the extract's biomolecules are responsible for reducing Ag^+ and Au^{3+} ions to Ag^0 and Au^0 to form nanoparticles and stabilize them in the extract. The present study confirmed that Ag, Au, and Ag-Au nanoparticles could be successfully synthesized in the aqueous bay leaf extract. These nanoparticles have potential usage in various applications, including the biomedical field.

ACKNOWLEDGMENTS

REFERENCES

1. Ding K, Cullen DA, Zhang L, Cao Z, Roy AD, Ivanov IN, et al. A general synthesis approach for supported bimetallic nanoparticles via surface inorganometallic chemistry. Science. 2018 Nov 2;362(6414):560–4. <DOI>.

2. Sankar M, Dimitratos N, Miedziak PJ, Wells PP, Kiely CJ, Hutchings GJ. Designing bimetallic catalysts for a green and sustainable future. Chem Soc Rev. 2012;41(24):8099. <DOI>.

3. Alonso DM, Wettstein SG, Dumesic JA. Bimetallic catalysts for upgrading of biomass to fuels and chemicals. Chem Soc Rev. 2012;41(24):8075. <DOI>.

4. Ferrando R, Jellinek J, Johnston RL. Nanoalloys: From Theory to Applications of Alloy Clusters and Nanoparticles. Chem Rev. 2008 Mar 1;108(3):845–910. <DOI>.

5. Chen HM, Liu RS, Jang L-Y, Lee J-F, Hu SF. Characterization of core–shell type and alloy Ag/Au bimetallic clusters by using extended X-ray absorption fine structure spectroscopy. Chemical Physics Letters. 2006 Apr;421(1–3):118–23. <DOI>.

6. Chatterjee K, Sarkar S, Jagajjanani Rao K, Paria S. Core/shell nanoparticles in biomedical applications. Advances in Colloid and Interface Science. 2014 Jul;209:8–39. <DOI>.

7. Kim K, Kim KL, Choi J-Y, Lee HB, Shin KS. Surface Enrichment of Ag Atoms in Au/Ag Alloy Nanoparticles Revealed by Surface-Enhanced Raman Scattering of 2,6-Dimethylphenyl Isocyanide. J Phys Chem C. 2010 Mar 4;114(8):3448–53. <DOI>.

8. Zhang L, Zhang J, Wang F, Shen J, Zhang Y, Wu L, et al. An Au@Ag nanocube based plasmonic nano-sensor for rapid detection of sulfide ions with high sensitivity. RSC Adv. 2018;8(11):5792–6. <DOI>.

9. Srnová-Šloufová I, Lednický F, Gemperle A, Gemperlová J. Core−Shell (Ag)Au Bimetallic Nanoparticles: Analysis of Transmission Electron Microscopy Images. Langmuir. 2000 Dec;16(25):9928–35. <DOI>.

10. Xu S, Zhao B, Xu W, Fan Y. Preparation of Au–Ag coreshell nanoparticles and application of bimetallic sandwich in surface-enhanced Raman scattering (SERS). Colloids and Surfaces A: Physicochemical and Engineering Aspects. 2005 May;257–258:313–7. <DOI>.

11. Mallik K, Mandal M, Pradhan N, Pal T. Seed Mediated Formation of Bimetallic Nanoparticles by UV Irradiation: A Photochemical Approach for the Preparation of "Core−Shell" Type Structures. Nano Lett. 2001 Jun 1;1(6):319–22. <DOI>.

12. Vinod M, Gopchandran KG. Ag@Au core–shell nanoparticles synthesized by pulsed laser ablation in water: Effect of plasmon coupling and their SERS performance. Spectrochimica Acta Part A: Molecular and Biomolecular Spectroscopy. 2015 Oct;149:913–9. <DOI>.

13. Philip D. Biosynthesis of Au, Ag and Au–Ag nanoparticles using edible mushroom extract. Spectrochimica Acta Part A: Molecular and Biomolecular Spectroscopy. 2009 Jul;73(2):374–81. <DOI>.

14. Shankar SS, Rai A, Ahmad A, Sastry M. Rapid synthesis of Au, Ag, and bimetallic Au core–Ag shell nanoparticles using Neem (Azadirachta

Hoda N et al. JOTCSA. 2021; 8(4): 1035-1044.

RESEARCH ARTICLE

indica) leaf broth. Journal of Colloid and Interface Science. 2004 Jul;275(2):496–502. <DOI>.

15. Kalaiarasi R, Jayallakshmi N, Venkatachalam P. Phytosynthesis of nanoparticles and its applications. Plant Cell Biotechnology and Molecular Biology. 2010;11(1/4):1–16.

16. Dwivedi AD, Gopal K. Biosynthesis of silver and gold nanoparticles using Chenopodium album leaf extract. Colloids and Surfaces A: Physicochemical and Engineering Aspects. 2010 Oct;369(1–3):27–33. <DOI>.

17. Song JY, Kim BS. Biological synthesis of bimetallic Au/Ag nanoparticles using Persimmon (Diopyros kaki) leaf extract. Korean J Chem Eng. 2008 Jul;25(4):808–11. <DOI>.

18. Sheny DS, Mathew J, Philip D. Phytosynthesis of Au, Ag and Au–Ag bimetallic nanoparticles using aqueous extract and dried leaf of Anacardium occidentale. Spectrochimica Acta Part A: Molecular and Biomolecular Spectroscopy. 2011 Jun;79(1):254–62. <DOI>.

19. Mondal S, Roy N, Laskar RA, Sk I, Basu S, Mandal D, et al. Biogenic synthesis of Ag, Au and bimetallic Au/Ag alloy nanoparticles using aqueous extract of mahogany (Swietenia mahogani JACQ.) leaves. Colloids and Surfaces B: Biointerfaces. 2011 Feb;82(2):497–504. <DOI>.

20. Zhan G, Huang J, Du M, Abdul-Rauf I, Ma Y, Li Q. Green synthesis of Au–Pd bimetallic nanoparticles: Single-step bioreduction method with plant extract. Materials Letters. 2011 Oct;65(19–20):2989–91. <DOI>.

21. Jacob J, Mukherjee T, Kapoor S. A simple approach for facile synthesis of Ag, anisotropic Au and bimetallic (Ag/Au) nanoparticles using cruciferous vegetable extracts. Materials Science and Engineering: C. 2012 Oct;32(7):1827–34. <DOI>.

22. Tamuly C, Hazarika M, Borah SCh, Das MR, Boruah MP. In situ biosynthesis of Ag, Au and bimetallic nanoparticles using Piper pedicellatum C.DC: Green chemistry approach. Colloids and Surfaces B: Biointerfaces. 2013 Feb;102:627–34. <DOI>.

23. AbdelHamid AA, Al-Ghobashy MA, Fawzy M, Mohamed MB, Abdel-Mottaleb MMSA. Phytosynthesis of Au, Ag, and Au–Ag Bimetallic Nanoparticles Using Aqueous Extract of Sago Pondweed (Potamogeton pectinatus L.). ACS Sustainable Chem Eng. 2013 Dec 2;1(12):1520–9. <DOI>.

24. Kasthuri J, Veerapandian S, Rajendiran N. Biological synthesis of silver and gold nanoparticles using apiin as reducing agent. Colloids and Surfaces B: Biointerfaces. 2009 Jan;68(1):55–60. <DOI>.

25. Boote BW, Byun H, Kim J-H. Silver–Gold Bimetallic Nanoparticles and Their Applications as Optical Materials. J Nanosci Nanotech. 2014 Feb 1;14(2):1563–77. <DOI>.

26. Hamidi-Asl E, Dardenne F, Pilehvar S, Blust R, De Wael K. Unique Properties of Core Shell Ag@Au Nanoparticles for the Aptasensing of Bacterial Cells. Chemosensors. 2016 Aug 29;4(3):16. <DOI>.

27. Nagaonkar D. Sequentially Reduced Biogenic Silver-Gold Nanoparticles With Enhanced Antimicrobial Potential Over Silver And Gold Monometallic Nanoparticles. AML. 2015 Apr 10;6(4):334–41. <DOI>.

28. Di Leo Lira P, Retta D, Tkacik E, Ringuelet J, Coussio JD, van Baren C, et al. Essential oil and by-products of distillation of bay leaves (Laurus nobilis L.) from Argentina. Industrial Crops and Products. 2009 Sep;30(2):259–64. <DOI>.

29. Sellami IH, Wannes WA, Bettaieb I, Berrima S, Chahed T, Marzouk B, et al. Qualitative and quantitative changes in the essential oil of Laurus nobilis L. leaves as affected by different drying methods. Food Chemistry. 2011 May;126(2):691–7. <DOI>.

30. Gómez-Coronado DJM, Barbas C. Optimized and Validated HPLC Method for α- and γ-Tocopherol Measurement in Laurus nobilis Leaves. New Data on Tocopherol Content. J Agric Food Chem. 2003 Aug;51(18):5196–201. <DOI>.

31. Dall'Acqua S, Viola G, Giorgetti M, Loi MC, Innocenti G. Two New Sesquiterpene Lactones from the Leaves of Laurus nobilis. Chem Pharm Bull. 2006;54(8):1187–9. <DOI>.

32. De Marino S, Borbone N, Zollo F, Ianaro A, Di Meglio P, Iorizzi M. Megastigmane and Phenolic Components from Laurus nobilis L. Leaves and Their Inhibitory Effects on Nitric Oxide Production. J Agric Food Chem. 2004 Dec;52(25):7525–31. <DOI>.

33. Fiorini C, David B, Fourasté I, Vercauteren J. Acylated kaempferol glycosides from Laurus nobilis leaves. Phytochemistry. 1998 Mar;47(5):821–4. <DOI>.

34. Sakar M, Engelshowe R. Monomere und dimere Gerbstoffvorstufen in Lorbeerblättern (Laurus

nobilis L.). Z Für Lebensm-Unters Forsch. 1985;180(6):494–5.

35. Baytop T. Therapy with medicinal plants in Turkey (past and present). Istanbul: Nobel Tıp Kitabevi; 2000.

36. Jha A, Prasad K. Understanding the involved mechanism in plant-mediated synthesis of nanoparticles. In: Rai M, Posten C, editors. Green biosynthesis of nanoparticles: mechanisms and applications. Wallingford, Oxfordshire ; Boston, Massachusetts: CABI; 2013. p. 122–31. ISBN: 978-1-78064-223-9.

37. Dias MI, Barros L, Dueñas M, Alves RC, Oliveira MBPP, Santos-Buelga C, et al. Nutritional and antioxidant contributions of Laurus nobilis L. leaves: Would be more suitable a wild or a cultivated sample? Food Chemistry. 2014 Aug;156:339–46. <DOI>.

38. Sinha SN, Paul D. Eco-friendly green synthesis and spectrophotometric characterization of silver nanoparticles synthesized using some common Indian spices. Int J Green Herbal Chem. 2014;3:401–8.

39. Vijayakumar S, Vaseeharan B, Malaikozhundan B, Shobiya M. Laurus nobilis leaf extract mediated green synthesis of ZnO nanoparticles: Characterization and biomedical applications. Biomedicine & Pharmacotherapy. 2016 Dec;84:1213–22. <DOI>.

40. Khalil M, Mahmoud I, Hamed M. Green synthesis of gold nanoparticles using Laurus nobilis L. leaf extract and its antimicrobial activity. Int J Green Herbal Chem. 2015;4(3):265–79.

41. Mulvaney P. Surface Plasmon Spectroscopy of Nanosized Metal Particles. Langmuir. 1996 Jan;12(3):788–800. <DOI>.

42. Yang Y, Shi J, Kawamura G, Nogami M. Preparation of Au–Ag, Ag–Au core–shell bimetallic nanoparticles for surface-enhanced Raman scattering. Scripta Materialia. 2008 May;58(10):862–5. <DOI>.

43. Gopinath K, Kumaraguru S, Bhakyaraj K, Mohan S, Venkatesh KS, Esakkirajan M, et al. Green synthesis of silver, gold and silver/gold bimetallic nanoparticles using the Gloriosa superba leaf extract and their antibacterial and antibiofilm activities. Microbial Pathogenesis. 2016 Dec;101:1–11. <DOI>.

44. Chavez K, Rosas G. Green Synthesis and Characterization of Ag@Au Core-shell Bimetallic Nanoparticles using the Extract of Hamelia patens Plant. Microsc Microanal. 2019 Aug;25(S2):1102–3. <DOI>.

45. Mukherjee P, Roy M, Mandal BP, Dey GK, Mukherjee PK, Ghatak J, et al. Green synthesis of highly stabilized nanocrystalline silver particles by a non-pathogenic and agriculturally important fungus T. asperellum. Nanotechnology. 2008 Feb 20;19(7):075103. <DOI>.

46. Dubey SP, Lahtinen M, Sillanpää M. Green synthesis and characterizations of silver and gold nanoparticles using leaf extract of Rosa rugosa. Colloids and Surfaces A: Physicochemical and Engineering Aspects. 2010 Jul;364(1–3):34–41. <DOI>.

47. Kumar VA, Ammani K, Jobina R, Subhaswaraj P, Siddhardha B. Photo-induced and phytomediated synthesis of silver nanoparticles using Derris trifoliata leaf extract and its larvicidal activity against Aedes aegypti. Journal of Photochemistry and Photobiology B: Biology. 2017 Jun;171:1–8. <DOI>.

48. Groiss S, Selvaraj R, Varadavenkatesan T, Vinayagam R. Structural characterization, antibacterial and catalytic effect of iron oxide nanoparticles synthesised using the leaf extract of Cynometra ramiflora. Journal of Molecular Structure. 2017 Jan;1128:572–8. <DOI>.

49. Nezamdoost T, Bagherieh-Najjar MB, Aghdasi M. Biogenic synthesis of stable bioactive silver chloride nanoparticles using Onosma dichroantha Boiss. root extract. Materials Letters. 2014 Dec;137:225–8. <DOI>.